Improvement of the Derjaguin-Broekhoff-de Boer Theory for the Capillary Condensation/Evaporation of Nitrogen in Spherical Cavities and Its Application for the Pore Size Analysis of Silicas with Ordered Cagelike Mesopores

Piotr Kowalczyk,*,†,‡ Mietek Jaroniec,*,§ Katsumi Kaneko,† Artur P. Terzyk,⊥ and Piotr A. Gauden⊥

Department of Chemistry, Faculty of Science, Chiba University, 1-3 Yayoi, Chiba, 263, Japan, Department III, Institute of Physical Chemistry, Polish Academy of Science, Kasprzaka Street 44/52, 01−224 Warsaw, Poland, Department of Chemistry, Kent State University, Kent, Ohio 44240, and Department of Chemistry, Physicochemistry of Carbon Materials Research Group, Nicolaus Copernicus University, Gagarin Street 7, 87−100 Torun, Poland

Received May 22, 2005. In Final Form: August 17, 2005

In a previous work, we proposed an improvement of the Derjaguin−Broekhoff−de Boer (DBdB) theory for capillary condensation/evaporation in open-ended cylindrical mesopores. In this paper, we report a further extension of this approach to the capillary condensation/evaporation of nitrogen in siliceous spherical cavities. The main idea of this improvement is to employ the Gibbs−Tolman−Koenig−Buff equation to predict the variation of the surface tension in spherical mesopores. In addition, the statistical film thickness (the so-called t-curve), which is evaluated accurately on the basis of adsorption isotherms measured for MCM-41 materials, is used instead of the originally proposed t-curve to take into account the excess chemical potential due to the surface forces. It is shown that the aforementioned modifications of the original DBdB theory that was refined by Ravikovitch and Neimark have significant implications for the pore size analysis of cagelike mesoporous silicas. To verify the proposed improvement of the DBdB pore size analysis (IDBdB), two series of FDU-1 samples, which are well-defined cagelike mesoporous materials (composed of siliceous spherical cavities interconnected by short necks), were used for the evaluation of the pore size distributions (PSDs). The correlation between the spinodal condensation point in the spherical pores predicted by the nonlocal density functional theory (NDFT) developed by Ravikovitch and Neimark and that predicted by the IDBdB theory is very good in the whole range of mesopores. This feature is mirrored to the realistic PSD characterized by the bimodal structure of pores computed from the IDBdB theory. As in the case of open-ended cylindrical pores, the improvement of the classical DBdB theory preserves its simplicity and simultaneously ensures a significant improvement of the pore size analysis, which is confirmed by the independent estimation of the average pore size by the NDFT and the powder X-ray diffraction method.

Introduction

It is commonly known that the wetting and capillary condensation/evaporation of adsorbates in pores is considerably affected by the pore geometry (cylindrical, spherical, slitlike, ink-bottle, etc.). Understanding the effect of the pore geometry on the wetting and capillary condensation/evaporation processes is important for the further advancement of adsorption theory and practice.[1−4] The cylindrical and spherical pore geometries are characteristic for several ordered mesoporous materials.[5−9] The ink-bottle pore geometry (i.e., the simplest model of the pore network) is usually modeled by the basic unit composed of the cylindrical necks (i.e., windows) attached to the main spherical cavity.[10−14] Both cylindrical and spherical geometries are characterized by strong confinement effects that cause a shift in the capillary condensation transition to the lower relative pressures compared to that of the flat surfaces.[15−18] The key issue in the gas adsorption characterization of the internal structures of a new generation of materials is the knowledge of phase equilibria in confined geometries. Obviously, the structure and properties of a fluid that is confined within a strong

* To whom correspondence should be addressed. E-mail: kowal@kora.ichf.edu.pl (P.K.); jaroniec@kent.edu (M.J.).
† Chiba University.
‡ Polish Academy of Science.
§ Kent State University.
⊥ Nicolaus Copernicus University.

(1) Neimark, A. V.; Ravikovitch, P. I.; Vishnyakov, A. *J. Phys.: Condens. Matter* **2003**, *15*, 347.
(2) Nicholson, D.; Parsonage, N. G. *Computer Simulation and the Statistical Mechanics of Adsorption*; Academic Press: London, 1982.
(3) Rouquerol, F.; Rouquerol, J.; Sing, K. S. W. *Adsorption by Powders and Porous Solids*; Academic Press: New York, 1999.
(4) Gubbins, K. E.; Quirke, N., Eds. *Molecular Simulation and Industrial Applications. Methods, Examples and Prospects*; Gordon and Breach Science Publishers: Singapore, 1996.
(5) Neimark, A. V.; Ravikovitch, P. I.; Grün, M.; Schüth, F.; Unger, K. K. *J. Colloid Interface Sci.* **1998**, *207*, 159.
(6) Kang, S.; Yu, J. S.; Kruk, M.; Jaroniec, M. *Chem. Commun.* **2002**, 1670.
(7) Qiao, S. Z.; Bhatia, S. K.; Nicholson, D. *Langmuir* **2004**, *20*, 389.
(8) Inoue, S.; Hanzawa, Y.; Kaneko, K. *Langmuir* **1998**, *14*, 3079.
(9) Olkhovyk, O.; Jaroniec, M. *J. Am. Chem. Soc.* **2005**, *127*, 60.
(10) Kruk, M.; Antochshuk, V.; Matos, J. R.; Mercuri, L. P.; Jaroniec, M. *J. Am. Chem. Soc.* **2002**, *124*, 768.
(11) Perez-Mendoza, M.; Gonzalez, J.; Wright, P. A.; Seaton, N. A. *Langmuir* **2004**, *20*, 7653.
(12) Perez-Mendoza, M.; Gonzalez, J.; Wright, P. A.; Seaton, N. A. *Langmuir* **2004**, *20*, 9856.
(13) Kruk, M.; Jaroniec, M. *Chem. Mater.* **2001**, *13*, 3169.
(14) Ravikovitch, P. I.; Neimark, A. V. *Langmuir* **2002**, *18*, 9830.
(15) Votyakov, E. V.; Tovbin, Y. K.; MacElroy, J. M. D.; Roche, A. *Langmuir* **1999**, *15*, 5713.
(16) Vishnyakov, A.; Piotrovskaya, E. M.; Brodskaya, E. N.; Votyakov, E. V.; Tovbin, Y. K. *Langmuir* **2001**, *17*, 4451.
(17) Evans, R.; Marconi Marini Bettolo, U.; Tarazona, P. *J. Chem. Soc., Faraday Trans. 2* **1986**, *82*, 1763.
(18) Röcken, P.; Tarazona, P. *J. Chem. Phys.* **1996**, *105*, 2034.

10.1021/la0513609 CCC: $30.25
Published on Web 10/05/2005

potential field generated by the pore walls differ significantly from those that are characteristic for the bulk fluid. For spherical pore geometry, the confinement effect is very high because of the strong solid−fluid interaction potential exposed by the pore walls.[19,20]

Molecular modeling methods, mainly grand canonical Monte Carlo (GCMC) simulations, gauge cell Monte Carlo simulations, nonlocal density functional theories (NDFTs), and molecular dynamics (MD), have been shown to be highly efficient tools for modeling the vapor−liquid equilibrium and the dynamics of adsorption/desorption in pores of various shapes.[2,21−24] However, making those methods applicable for the analysis of porous systems with strongly heterogeneous surfaces is a very challenging task, which requires further advancement in statistical thermodynamics and computer programming. For mesopores with heterogeneous walls, such as those present in ordered silicas, the elaboration of effective Monte Carlo (MC), MD, and density functional theory (DFT) methods seems to be very difficult because of the dimensions of the simulation system and the challenge of properly representing interfacial heterogeneity. In addition, computer simulation results do not provide the analytical model of adsorption, as pointed out by Rudzinski and Cerofolini.[25]

On the other hand, classical phenomenological approaches with proper model formulation are still applicable for the modeling of capillary condensation/evaporation in mesopores.[26−30] Ordered mesoporous materials, including the silica-type materials, are the most widespread and are suitable for the verification and improvement of the classical thermodynamics methods.[31−34] The simplified pore models, such as uniform spheres and open-ended cylinders, inadequately describe real porous media, which are characterized by an enormously complex pore structure (i.e., activated carbons, porous glasses, silica gels, etc.). However, the simplification gained by treating the pores in novel ordered siliceous materials as uniform cylinders or spheres is fully justified because their detailed pore geometry and arrangement can be independently observed by other experimental techniques.[35−38] In fact, the discovery of ordered mesoporous silicas revealed and/or confirmed some new features of the confined fluids (i.e., shift in the critical freezing temperature compared to that of the bulk fluid, impact of the pore size, adsorbate, and temperature on the hysteresis loop appearance, etc.).[1,39,40]

The tailored pore size of new ordered materials reveals that the classical phenomenological approaches fail when the size of the pore is comparable to several adsorbed molecular layers.[41,42] In a series of papers, Neimark et al. established criteria for the applicability of the phenomenological approaches, including the Derjaguin-Broekhoff-de Boer (DBdB) theory, which is the most sophisticated approach.[1,20] The remaining methods, such as the most widespread method proposed by Barrett−Joyner−Halenda (BJH), fail to predict the capillary condensation/evaporation curves, especially for spherical/cylindrical pore radii smaller 5 nm.[20,42] In 1997, Kruk et al. used a series of MCM-41 samples to develop a practical method to calculate the pore size distribution (PSD) for adsorbents with open-ended cylindrical mesopores.[26] The empirical improvement of the classical BJH method is a remarkable improvement of the PSD analysis; however it is restricted to open-ended cylindrical pore geometry and the pore diameter calibration range obtained from X-ray diffraction (XRD). Moreover, Kruk et al. recommended the use of the adsorption branch of the hysteresis loop for the PSD analysis. In 2005, Ustinov et al.[43] proposed a modification of both the continuum Broekhoff−de Boer (BdB) theory, called the curvature-dependent potential-Broekhoff−de Boer (CDP-BdB) theory, and the NDFT for capillary condensation/evaporation in open-ended cylindrical pore geometries with amorphous surfaces. Moreover, Ustinov et al. showed that the PSD obtained from the adsorption branch of the experimental hysteresis loop (MCM-41 and SBA-15 silica materials) by the CDP-BdB theory and that obtained by the NDFT approach coincide.

Here, we present an improvement of the DBdB theory for capillary condensation/evaporation in spherical cavities. This paper is a further extension of our previous work, in which the DBdB theory of capillary condensation/evaporation in open-ended cylindrical pores was improved.[42] The primary idea of this improvement was to employ the Gibbs−Tolman−Koenig−Buff (GTKB) equation to predict the dependence of surface tension on pore size. In addition, the statistical film thickness (the so-called t-curve), which is accurately evaluated on the basis of adsorption isotherms measured for MCM-41 materials, was used instead of the originally proposed t-curve (to take into account the excess chemical potential due to the surface forces).[42] We proved that the aforementioned modifications to the original DBdB theory have significant implications in the pore size analysis of mesoporous solids. The agreement between the so-called improved DBdB (IDBdB) theory and the most sophisticated nonlocal version of the density functional theory (NDFT) implemented by Neimark et al. according to Tarazona's scheme, was observed in the whole range of the relative pressure for the capillary condensation curve.[42] Moreover, the mean pore size calculated by the IDBdB approach was correlated

(19) Henderson, D.; Sokolowski, S. *Phys. Rev. E* **1995**, *52*, 758.
(20) Ravikovitch, P. I.; Neimark, A. V. *Langmuir* **2002**, *18*, 1550.
(21) Pikunic, J.; Clinard, C.; Cohaut, N.; Gubbins, K. E.; Guet, J. M.; Pellenq, R. J. M.; Rannou, I.; Rouzaud, J. N. *Langmuir* **2003**, *19*, 8565.
(22) Ravikovitch, P. I.; Vishnyakov, A.; Neimark, A. V. *Phys. Rev. E* **2001**, *64*, 011602.
(23) Frenkel, D.; Smit, B. *Understanding Molecular Simulation: From Algorithms to Applications*; Academic Press: New York, 1996.
(24) Allen, M. P.; Tildesley, D. J. *Computer Simulation of Liquids*; Clarendon Press: Oxford, U.K., 1987.
(25) Rudzinski, W.; Steele, W. A.; Zgrablich, G. *Stud. Surf. Sci. Catal.* **1997**, *104*, 1.
(26) Kruk, M.; Jaroniec, M.; Sayari, A. *Langmuir* **1997**, *13*, 6267.
(27) Gauden, P. A.; Kowalczyk, P.; Terzyk, A. P. *Langmuir* **2002**, *19*, 4253.
(28) Kowalczyk, P.; Gun'ko, V. M.; Terzyk, A. P.; Gauden, P. A.; Rong, H.; Ryu, Z.; Do, D. D. *Appl. Surf. Sci.* **2003**, *206*, 67.
(29) Kowalczyk, P.; Terzyk, A. P.; Gauden, P. A.; Leboda, R.; Szmechtig-Gauden, E.; Rychlicki, G.; Ryu, Z.; Rong, H. *Carbon* **2003**, *41*, 1113.
(30) Terzyk, A. P.; Gauden, P. A.; Kowalczyk, P. *Carbon* **2002**, *40*, 2879.
(31) Ravikovitch, P. I.; Neimark, A. V. *J. Phys. Chem. B* **2001**, *105*, 6917.
(32) Ravikovitch, P. I.; Neimark, A. V. *Stud. Surf. Sci. Catal.* **2000**, *129*, 597.
(33) Qiao, S. Z.; Bhatia, S. K.; Zhao, X. S. *Microporous Mesoporous Mater.* **2003**, *65*, 287.
(34) Neimark, A. V.; Ravikovitch, P. I. *Microporous Mesoporous Mater.* **2001**, *44−45*, 697.
(35) Kresge, C. T.; Leonowicz, M. E.; Roth, W. J.; Vartuli, J. C.; Beck, J. S. *Nature* **1992**, *359*, 710.
(36) Inagaki, S.; Koiwai, A.; Suzuki, N.; Fukushima, Y.; Kuroda, K. *Bull. Chem. Soc. Jpn.* **1996**, *69*, 1449.
(37) Yanagisawa, T.; Shimizu, T.; Kuroda, K.; Kato, Ch. *Bull. Chem. Soc. Jpn.* **1990**, *63*, 988.
(38) Yanagisawa, T.; Shimizu, T.; Kuroda, K.; Kato, Ch. *Bull. Chem. Soc. Jpn.* **1990**, *63*, 1535.
(39) Morishige, K.; Nakamura, Y. *Langmuir* **2004**, *20*, 4503.
(40) Gelb, L. D.; Gubbins, K. E.; Radhakrishnan, R.; Sliwinska-Bartkowiak, M. *Rep. Prog. Phys.* **1999**, *62*, 1573.
(41) Ravikovitch, P. I.; Neimark, A. V. *Colloids Surf., A* **2001**, *187−188*, 11.
(42) Kowalczyk, P.; Jaroniec, M.; Terzyk, A. P.; Kaneko, K.; Do, D. D. *Langmuir* **2005**, *21*, 1827.
(43) Ustinov, E. A.; Do, D. D.; Jaroniec, M. *J. Phys. Chem. B* **2005**, *109*, 1947.

with one obtained from powder XRD. It is worth pointing out that the IDBdB approach combined with the Dollimore−Heal method generates a position and dispersion of the PSD of MCM-41 samples that is very close to that published by Kruk et al.[42]

There is another important group of ordered siliceous materials that have cagelike structures.[44−47] As we mentioned above, the structure of cagelike mesoporous silicas can be modeled as classical ink-bottle pore geometry with a basic unit composed of short cylindrical necks attached to the main spherical cavity. FDU-1 and SBA-16 are the most popular cagelike mesoporous silicas.[48,49] The connectivity (i.e., the number of necks attached to the basic unit) is the characteristic feature of these materials. For instance, the basic unit of the FDU-1 cagelike mesoporous silica consists of twelve cylindrical necks attached to the main spherical cavity, whereas, for SBA-16, the number of cylindrical necks is eight. Moreover, the intrawall micropores, which are the consequence of using triblock copolymers as the template, are well-documented characteristic features of the above-mentioned silica materials.[48,49]

Because the main spherical cavity is an important element of ink-bottle pore geometry, in this paper, the improvement of the classical DBdB theory for capillary condensation/evaporation in spherical cavities is presented for the first time. Similar to Ravikovitch and Neimark,[20] we assumed that the adsorption branch of the experimental hysteresis loop in ink-bottle pore geometry corresponds to the spontaneous spinodal condensation of the fluid in the main spherical cavities. Thus, the capillary condensation condition is determined by the size of the spherical cavity. It is well-documented that, for the ink-bottle pore, the desorption mechanism is not unique. Generally speaking, three mechanisms for the desorption of adsorbed molecules from the ink-bottle pore can be distinguished.[50] First, the desorption of the adsorbed molecules from the central part of the ink-bottle pore (i.e., from the spherical cavity) can be controlled by the size of the attached cylindrical necks (i.e., the classical pore-blocking mechanism).[51] Second, spontaneous evaporation is caused by a cavitation of the stretched metastable liquid. Finally, desorption takes place by the mechanism of near-equilibrium evaporation in the region of the hysteresis from unblocked cavities having access to the vapor phase.[50]

Similar to that of Ustinov et al.,[43] our PSD analysis is based on the adsorption branch of the experimental hysteresis loop because of the reasons mentioned above. Here we want to point out that the desorption mechanism in ink-bottle pore geometry can either obey or not obey the classical DBdB scenario. Consequently, the distribution of the necks theoretically related to the desorption branch of the experimental hysteresis loop can be unrealistic.

The manuscript is organized as follows: In the next part we present the final equations derived on the basis of the IDBdB theory for spherical pore geometry. For the sake of clarity, the main assumptions introduced previously for open-ended pore geometry are reintroduced. Additionally, the numerical algorithm used for the analysis of the PSD from a single gas adsorption isotherm of nitrogen at 77 K is described. Next, the experimental verification of the new proposal is presented. To do this, the PSD of FDU-1 cagelike mesoporous silicas are determined and compared with those obtained by other experimental methods.

IDBdB Theory

An improvement of the classical DBdB theory for capillary condensation/evaporation in open-ended cylindrical capillaries was presented in our previous work.[42] Here, we reintroduce the main ideas of the IDBdB theory and present its extension for the capillary condensation/evaporation in spherical mesopores.

It was previously shown that the experimental adsorption data for a reference flat silica surface can be properly described by using the disjoining pressure isotherm in the form[42]

$$\Pi_1 \exp(-h/\lambda_1) + \Pi_2 \exp(-h/\lambda_2) = -(RT/v_m) \ln(p/p_0) \quad (1)$$

in which Π_1 and Π_2 characterize the strength of the surface forces field, whereas the parameters λ_1 and λ_2 are responsible for the range of the structural forces action. Clearly, the first term dominates in thick adlayers, whereas the second term dominates in thin adlayers. All of the parameters appearing in eq 1 were tabulated previously for the adsorption of argon and nitrogen at their boiling points on the selected reference silica surface.[42]

The critical radius, at which a spontaneous capillary condensation occurs (i.e., spinodal condensation point), is closely related to the assumed pore geometry. For the wetting films formed on a concave surface of spherical pores, the following relationship is valid:[20]

$$\Pi(h) = \Pi_1 \exp(-h/\lambda_1) + \Pi_2 \exp(-h/\lambda_2) + \frac{2\gamma(r_m)}{r-h} = -(RT/v_m) \ln(p/p_0) \quad (2)$$

As demonstrated previously, the surface tension of a liquid adsorbate (see eq 2) depends on the meniscus radii $r_m = r - h$, which seems to be particularly important for the pores at the borderline between micropores and mesopores.

Similar to the work completed by Miyahara and coworkers,[52] the GTKB was used in this work. The GTKB equation for the cylindrical interface (capillary condensation) can be written as follows:[42]

$$\frac{\gamma(r_m)}{\gamma_\infty} = 1 - \frac{\delta}{r_m} \quad (3)$$

In eq 3, γ_∞ denotes the surface tension of the bulk fluid, and δ is the displacement of the surface at zero mass density relative to the tension surface. The physical meaning of δ and its impact on the spinodal condensation point was presented previously.

The stability condition of the wetting film was formulated earlier by Derjaguin et al. as $d\Pi(h)dh < 0$. Obviously,

(44) Kruk, M.; Celer, E. B.; Jaroniec, M. *Chem. Mater.* **2004**, *16*, 698.
(45) Matos, J. R.; Kruk, M.; Mercuri, L. P.; Jaroniec, M.; Asefa, T.; Coombs, N.; Ozin, G. A.; Kamiyama, T.; Terasaki, O. *Chem. Mater.* **2002**, *14*, 1903.
(46) Kruk, M.; Celer, E. B.; Matos, J. R.; Pikus, S.; Jaroniec, M. *J. Phys. Chem. B* **2005**, *109*, 3838.
(47) Matos, J. R.; Mercuri, L. P.; Kruk, M.; Jaroniec, M. *Langmuir* **2002**, *18*, 884.
(48) Kim, T. W.; Ryoo R.; Kruk, M.; Gierszal, K. P.; Jaroniec, M.; Kamiya, S.; Terasaki, O. *J. Phys. Chem. B* **2004**, *108*, 11480.
(49) Matos, J. R.; Kruk, M.; Mercuri, L. P.; Jaroniec, M.; Zhao, L.; Kamiyama, T.; Terasaki, O.; Pinnavaia, T. J.; Lin., Y *J. Am. Chem. Soc.* **2003**, *125*, 821.
(50) Vishnyakov, A.; Neimark, A. V. *Langmuir* **2003**, *19*, 3240.
(51) Everett, D. H. In *The Solid−Gas Interface*; Flood, E. A., Ed.; Marcel Dekker: New York, 1967; Vol. 2, Chapter 36, p 1055.
(52) Kanda, H.; Miyahara, M.; Yoshioka, T.; Okazaki, M. *Langmuir* **2000**, *16*, 6622.

both the critical film thickness, h_{cr}, and the critical capillary radius, r_{cr}, corresponding to the film collapse, are determined from[42]

$$\frac{d\Pi(h)}{dh}|_{h=h_{cr},r=r_{cr}} = 0 \quad (4)$$

The condition given by eq 4 determines the spontaneous spinodal condensation when the adsorbed film thickness becomes mechanically unstable.

A combination of eqs 1−4 gives the relation between both the critical film thickness and the critical capillary radius as a function of the relative pressure for the spherical pore geometry:

$$\begin{cases} \dfrac{2\gamma_\infty(r-h-2\delta)}{(r-h)^3} - \dfrac{\Pi_1}{\lambda_1}\exp(-h/\lambda_1) - \dfrac{\Pi_2}{\lambda_2}\exp(-h/\lambda_2) = 0 \\ \dfrac{2\gamma_\infty(r-h-\delta)}{(r-h)^2} + \Pi_1\exp(-h/\lambda_1) + \Pi_2\exp(-h/\lambda_2) = -(RT/v_m)\ln(p/p_0) \end{cases} \quad (5)$$

The solution of this system of algebraic equations can be obtained by chord or other standard numerical procedures.

The desorption from the considered spherical cavity is determined by the condition of the formation of the equilibrium meniscus given by the augmented Kelvin equation, known as the Derjaguin equation:[20]

$$RT\ln(p_0/p) = \frac{3v_m\gamma_\infty\left(1-2\dfrac{\delta}{r-h_e}\right) + \dfrac{3v_m}{(r-h_e)^2}\displaystyle\int_{h_e}^{r}(r-h)^2\Pi(h)dh}{r-h_e} \quad (6)$$

In eq 6, similar to the work completed by Miyahara and co-workers, the GTKB equation for the spherical interface is introduced. The thickness of the adsorbed film in equilibrium with the meniscus (h_e) for the spherical pore is given by

$$RT\ln(p_0/p) = \Pi(h_e)v_m + \frac{2v_m\gamma_\infty\left(1-\dfrac{\delta}{r-h_e}\right)}{r-h_e} \quad (7)$$

For constant surface tension, eqs 5−7 reduce to the classical DBdB equations, which are described in the series of papers published by Ravikovitch and Neimark.[20]

For application purposes, we can derive the analytical formulas for the calculation of the equilibrium transition in the considered spherical pore geometry according to eqs 6 and 7.

As we mentioned above, for the spherical pore, the system of equations describing the equilibrium desorption transition is defined by the following relation:

$$\begin{cases} \ln(p/p_0) = [\Pi_1\exp(-h_e/\lambda_1) + \Pi_2\exp(-h_e/\lambda_2)]\dfrac{v_m}{RT} + \dfrac{2\gamma_\infty v_m\left(1-\dfrac{\delta}{r-h_e}\right)}{RT(r-h_e)} \\ \ln(p/p_0) = \dfrac{3\dfrac{\gamma_\infty\left(1-2\dfrac{\delta}{r-h_e}\right)}{RT} + 3\dfrac{v_m}{RT(r-h_e)}[\zeta_1+\zeta_2]}{r-h_e} \end{cases} \quad (8)$$

in which the coefficients ζ_1 and ζ_2 are given by the following formulas:

$$\zeta_1 = \Pi_1\lambda_1\{-2\lambda_1^2\exp(-r/\lambda_1) + \exp(-h_e/\lambda_1)[2\lambda_1(\lambda_1 + h_e - r) + (r-h_e)^2]\} \quad (9)$$

$$\zeta_2 = \Pi_2\lambda_2\{-2\lambda_2^2\exp(-r/\lambda_2) + \exp(-h_e/\lambda_2)[2\lambda_2(\lambda_2 + h_e - r) + (r-h_e)^2]\} \quad (10)$$

As can be seen from the above equations for spherical pore geometry, the final system of equations describing spontaneous capillary condensation (eq 5) and the equilibrium desorption transition (eq 8) are the classical Kelvin equations, corrected for the surface forces and varying surface tension according to the GTKB equations.

As we pointed out previously, our improvement of the standard DBdB theory does not include any additional fitting parameters, and it is thermodynamically correct. These equations reduce to the classical Kelvin or DBdB theories under some assumptions. In the next part of this paper, we will prove the utility of this improvement. As we suspect from our previous studies, for the small spherical pores, the effect of the surface tension changes is dominant and significantly influences the relation between both the spontaneous capillary condensation and the equilibrium desorption versus the relative pressure. Obviously, for larger spherical capillaries, the current version of the DBdB theory reduces to the classical theory, according to the results of Ravikovitch and Neimark,[20] because the surface tension within the pore approaches that in the bulk phase.

In our previous study, we pointed out the weak points of the IDBdB method. Additionally, as we pointed out above, the classical scenario of desorption from the ink-bottle pore geometry (incorporated to the DBdB theory) is not a unique mechanism. Consequently, the adopted classical concept of the pore-blocking mechanism in the ink-bottle pore geometry can generate enormous PSDs of the necks, applying the desorption branch of the experimental hysteresis loop. For this reason, we concentrate on the evaluation of the PSD curve from the adsorption branch of the experimental hysteresis loop (i.e., the PSD of the spherical cavities).

Because of the structural heterogeneities, the PSD of spherical cavities can be represented as a combination of the theoretical isotherms in individual pores (i.e., the linear Fredholm integral equation of the first kind):[27−30,53−56]

(53) Jaroniec, M.; Madey, R. *Physical Adsorption on Heterogeneous Solids*; Elsevier: Amsterdam, 1988.
(54) Rudzinski, W.; Everett, D. H. *Adsorption of Gases on Heterogeneous Surfaces*; Academic Press: New York, 1992.
(55) Do, D. D. *Adsorption Analysis: Equilibria and Kinetics*; Imperial College Press: London, 1998.
(56) Kowalczyk, P.; Terzyk, A. P.; Gauden, P. A. *Langmuir* **2002**, *18*, 5406.

$$\theta_{exp}(h) = \int_{\Omega(D)} \theta_{loc}(D_{in},h)\chi(D_{in})dD_{in} \qquad (11)$$

Here,

$$\theta_{loc}(D_{in},h) = \begin{Bmatrix} t/t_{cr}, & t < t_{cr} \\ 1, & \text{elsewhere} \end{Bmatrix}$$

represents the kernel of the theoretical isotherms generated from the IDBdB approach in pores of different diameters, D_{in}, and $\chi(D_{in})$ is the normalized differential PSD function.

As mentioned above, the kernel of the integral equation (given by eq 11) was obtained assuming there is spinodal condensation in the spherical pores (described by eq 5). In this paper, we solved eq 11 in its discreet form by applying (as proposed by us previously) the ASA algorithm along with the stabilizing first-order Tihkonov's regularization term.[27−30,42,56,57] The regularization parameter was selected through a series of trials by an interactive judgment of the solution. During the regularization, some of the artificial shoulders and stairs were smoothed out.

Results and Discussion

In the preceding section, the general formulas for spherical pore geometry were introduced using the IDBdB theory. We want to point out that the solutions for all of the derived equations are computationally simple and very fast, compared to the advanced methods based on statistical thermodynamics (i.e., NDFT or GCMC). Unfortunately, eq 11, like other linear Fredholm equations of the first kind, belongs to a group of so-called "ill-posed" problems.[58] The standard numerical treatment of eq 11 cannot be applied because of the large matrix singularity (i.e., high sensitivity to any experimental errors and so on); however, the problem can be successfully solved applying (as proposed by us) the ASA method with the static penalty function (i.e., additional Tihkonov's regularization term).[27−30,42,56,57]

As we mentioned above, like Ravikovitch and Neimark,[20] we assumed that the model of the spherical pore geometry was adequate for the modeling of the adsorption process in the cagelike siliceous materials. Roughly speaking, it is assumed that during adsorption, the isotherm traces a sequence of metastable states of the adsorbed film, and the capillary condensation occurs spontaneously when the thickness approaches the limit of the stability. Thus, the point of the vaporlike spinodal relates to the size of the siliceous sphere. In this paper, eqs 5 and 8 (describing the capillary condensation/evaporation in the spherical cavities) were solved for low-temperature nitrogen adsorption/desorption by using the following parameters: $\sigma_{ff} = 0.3681$ nm, $\gamma_\infty = 8.88 \times 10^{-3}$ N/m, $V_m = 34.68$ cm^3/mol, and $T = 77$ K. Table 1 contains numerical data for the capillary condensation pressure in spherical siliceous cavities expressed as a function of the pore diameter. These data can be used to find the pore diameter corresponding to the capillary condensation pressure estimated from the low-temperature nitrogen adsorption data. Obviously, the presented dependence makes it possible to easily estimate the average size of the central spherical siliceous cavity, whereas the rigorous estimation of the heterogeneity effect requires the solution of eq 11.

At first, Figure 1 shows the prediction of the capillary condensation/evaporation pressure in a spherical siliceous cavity by the classical DBdB approach refined by Ravikovitch and Neimark, the NDFT formulated by Ravikovitch and Neimark, and the IDBdB method.[20] As in the case of the fully open-ended cylindrical mesopores, the IDBdB theory (adopted for spherical geometry) considerably shifts the relations compared to the classical theories for a siliceous spherical cavity diameter smaller than 10 nm. On the other hand, the asymptotic correlation between the classical DBdB approach and the IDBdB was observed for higher values of the siliceous spherical pore diameter. Additionally, the correlation between the capillary condensation pressure evaluated from the IDBdB method and that evaluated from the NDFT method was found to be very good in the whole range of the siliceous spherical pore diameter. Conversely, the capillary evaporation curve asymptotically approaches the NDFT prediction, and the correlation is observed for the siliceous pore diameter $D > 15$ nm. The coincidence of the condensation and evaporation (i.e., the reversibility of the experimental isotherm) curves in the range of the small pore diameters is not observed for both the classical and the IDBdB method, which can be attributed to the limitation of the phenomenological thermodynamics.

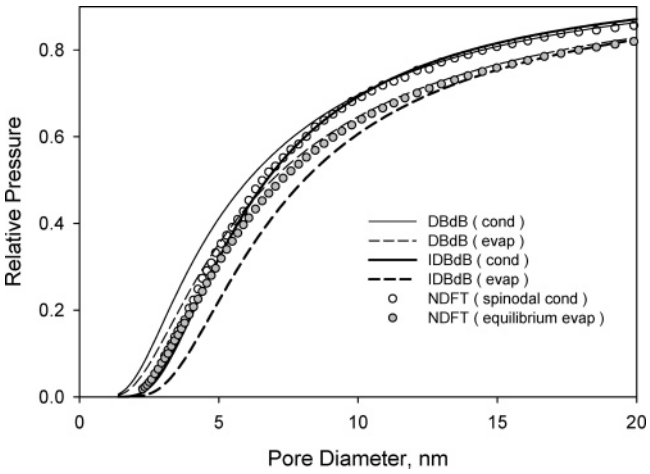

Figure 1. The relations between the capillary condensation/evaporation pressure and the pore diameter for the spherical siliceous cavity obtained from the DBdB, IDBdB, and NDFT theories.

Table 1. Values of the Capillary Condensation Pressure (p/p_0) and the Corresponding Pore Diameter for Nitrogen in the Spherical Siliceous Cavity at 77 K, Calculated by the IDBdB Method

w_{silica} (nm)	p/p_0	w_{silica} (nm)	p/p_0	w_{silica} (nm)	p/p_0
2.000	0.003	11.492	0.742	20.983	0.878
2.475	0.020	11.966	0.755	21.458	0.882
2.949	0.056	12.441	0.767	21.932	0.885
3.424	0.109	12.915	0.777	22.407	0.888
3.898	0.171	13.390	0.787	22.881	0.891
4.373	0.236	13.864	0.797	23.356	0.893
4.847	0.299	14.339	0.805	23.831	0.896
5.322	0.358	14.814	0.813	24.305	0.898
5.797	0.412	15.288	0.820	24.780	0.901
6.271	0.460	15.763	0.827	25.254	0.903
6.746	0.502	16.237	0.833	25.729	0.905
7.220	0.540	16.712	0.839	26.203	0.907
7.695	0.574	17.186	0.845	26.678	0.909
8.169	0.604	17.661	0.850	27.153	0.911
8.644	0.630	18.136	0.855	27.627	0.913
9.119	0.654	18.610	0.859	28.102	0.914
9.593	0.676	19.085	0.863	28.576	0.916
10.068	0.695	19.559	0.867	29.051	0.918
10.542	0.712	20.034	0.871	29.525	0.919
11.017	0.728	20.508	0.875	30.000	0.921

(57) Morozov, V. A. *Methods for Solving Incorrectly Posed Problems*; Springer: Berlin, 1984.
(58) Kowalczyk, P.; Tanaka, H.; Kanoh, H.; Kaneko, K.; *Langmuir* **2004**, *20*, 2324.

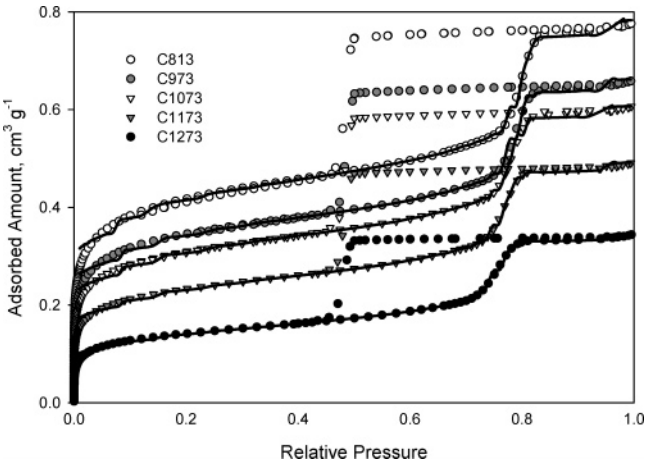

Figure 2. Nitrogen adsorption isotherms for FDU-1 silica samples calcined at different temperatures. The points correspond to the experimental data,[44] and the lines represent the theoretical fitting obtained by the IDBdB method.

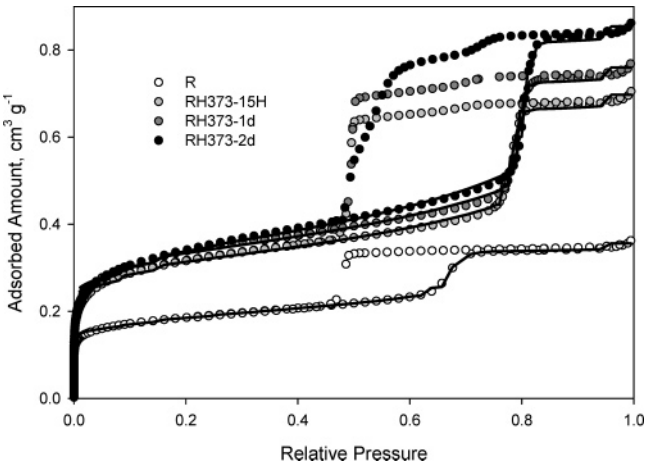

Figure 3. Nitrogen adsorption isotherms (at 77 K) for FDU-1 silica samples synthesized in the presence of NaCl in the synthesis mixture. The points correspond to the experimental data,[46] and the lines represent the theoretical fitting obtained by the IDBdB method.

Until now, we focused on the prediction of the capillary condensation/evaporation curves for the spherical pore geometry by using the IDBdB approach. However, the most important problem is the estimation of the heterogeneity effect. As we mentioned above, eq 11 can be used for the estimation of the PSD from the single gas adsorption isotherm. For the validation of this improvement of the DBdB theory, we used adsorption data for two series of cagelike siliceous FDU-1 materials, which were reported elsewhere.[44,46] Our first examination of the IDBdB method combined with eq 11 was employed for a series of FDU-1 cagelike silicas calcined at different temperatures. For both series, the isotherms were characterized by the H2-type hysteresis loops according to the IUPAC classification (see Figures 2 and 3). They are broad with a long and almost flat plateau and a steep desorption branch. The H2-type experimental hysteresis loops are usually observed for the interconnected network of pores of different sizes and shapes (i.e., in the simplest treatment, they are modeled by ink-bottle pore geometry).

Because our model is based on the phenomenological thermodynamics, we restricted the fitting of the nitrogen experimental adsorption isotherm to $p/p_0 > 0.05$. The theoretical description of the experimental nitrogen isotherms on the FDU-1 samples is shown in Figures 2 and 3. From these figures, one can conclude that the theoretical description of the experimental data is good. The small scattering of the theoretical points at low pressures can be attributed to the assumed discreet form of PSD; however, we can suspect that this characteristic of the fitting line does not have a considerable influence on the shape of the PSD curves. Figures 4 and 5 confirm our hypothesis. The resulting PSDs are characterized by almost symmetrical smooth two peaks. The first peak can be attributed to the size of the pore entrance and intrawall microporosity. Notice, that the position and dispersion of the first peak are almost the same for all of the samples studied. Here, we want to point out that properly describing the experimental adsorption isotherm while neglecting the presence of the first peak is impossible. The second peak on the PSD represents the size distribution of the main siliceous spherical cavities. The intensity, position, and dispersion of this peak vary for the samples studied. A systematic shift and lowering of the second peak reflects differences between the samples studied.

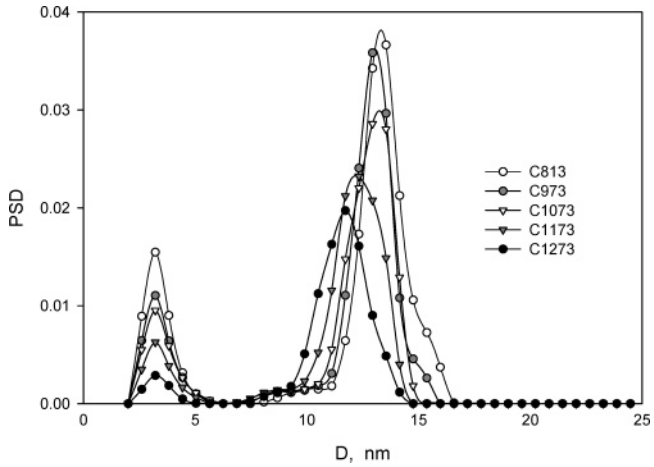

Figure 4. PSDs evaluated from nitrogen adsorption isotherms at 77 K by the IDBdB method for FDU-1 silica samples calcined at different temperatures.

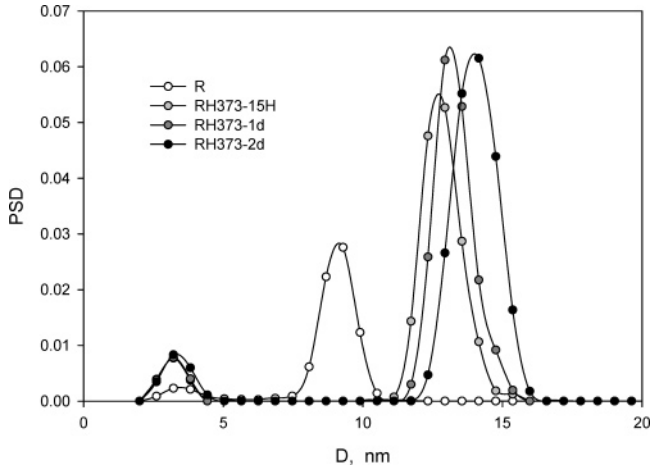

Figure 5. PSDs evaluated by the IDBdB method for FDU-1 silica samples (determined from nitrogen adsorption isotherms at 77 K) synthesized in the presence of NaCl in the synthesis mixture.

It should be mentioned that the second peak of the PSD is evaluated with high accuracy because the IDBdB model developed for spheres was used to analyze the spherical mesopores in the FDU-1 samples. This is not the case for the first peak of the PSD, which represents small interconnections between ordered spherical mesopores and irregular intrawall microporosity. Analysis of those fine

Table 2. The Structural Properties of FDU-1 Silica Samples Synthesized in the Presence of NaCl in the Synthesis Mixture[a]

	sample code			
parameter	R	RH373−15H	RH373−1d	RH373−2d
V_{total} (cm^3/g)	0.36	0.70	0.76	0.86
V_{mez} (cm^3/g)	0.22	0.48	0.54	0.64
D_{XRD} (nm)	9.6	12.2	12.8	13.6
D_{NDFT} (nm)	9.21	13.25	13.97	14.86
D_{mic} (nm)	3.75	3.21	3.23	3.37
D_{mez} (nm)	9.10	12.86	13.28	14.03
δ_{mic}	0.14	0.12	0.12	0.15
δ_{mez}	0.23	0.31	0.32	0.36

[a] Abbreviations: V_{total} = total pore volume calculated from the nitrogen liquid density at $p/p_0 \cong 0.99$; V_{mez} = total volume of the spherical cavities obtained from the integration of the main peak in the PSD; D_{XRD} = average pore size of the spherical cavities calculated from the XRD measurements using the equation provided in ref 49; D_{NDFT} = average pore size of the spherical cavities obtained from the Ravikovitch−Neimark NDFT spinodal condensation; D_{mic} = average pore size calculated from the IDBdB method for the pore entrance/intrawall micropores; D_{mez} = average pore size of the spherical cavities calculated from the IDBdB method; δ_{mic}, δ_{mez} = standard deviations of the first and second peaks of the PSD calculated from the IDBdB method, respectively.

pores by the IDBdB model developed for spheres is less accurate because their shape is rather cylindrical. Because the pore size analysis of any system having pores of different geometries is a very difficult and is an unsolved issue, it seems logical to analyze such porous system by a method that is applicable for the dominating pores. Therefore, the use of the IDBdB method for the analysis of the systems studied is justified because in these systems spherical cages are the dominating (primary) mesopores.

The comparison of the pore size obtained from the IDBdB, the NDFT (average spherical cavity diameter estimated from the inflection point of the adsorption branch of the nitrogen isotherm), and XRD is summarized in Tables 2 and 3. As can be seen from these tables, the prediction of the average diameter of the siliceous spherical

Table 3. Structural Properties of FDU-1 Silica Samples Calcined at Different Temperatures

	sample code				
parameter	C813	C973	C1073	C1173	C1273
V_{total} (cm^3/g)	0.77	0.66	0.61	0.49	0.34
V_{mez} (cm^3/g)	0.44	0.39	0.37	0.33	0.27
D_{NDFT} (nm)	14.57	13.99	13.41	12.91	12.68
D_{mez} (nm)	13.35	12.85	12.66	12.13	11.59
D_{mic} (nm)	3.38	3.41	3.48	3.44	3.35
δ_{mez}	0.49	0.46	0.47	0.45	0.39
δ_{mic}	0.26	0.23	0.24	0.17	0.10

cavities by the most sophisticated methods of the porosity analysis fully validate the currently proposed method.

Summarizing our results, we can state that the current proposal significantly improves the pore size analysis of cagelike mesoporous silicas. The proposed modification of the standard DBdB theory refined by Ravikovitch and Neimark[20] strongly influences the relations for the capillary condensation/evaporation in spherical cavities with small pore diameters. The bimodal structure of the cagelike silica samples studied that was predicted by the IDBdB approach is in agreement with other experimental studies. The size distribution of the pore entrance/intrawall microporosity is not strongly affected by the synthesis employing triblock copolymers as templates. On the other hand, the size distribution of the main spherical cavities is sensitive to the synthesis conditions and can be tuned.

The proposed improvement of the DBdB theory seems to be a very useful tool for the characterization of the internal structure of cagelike mesoporous silicas and related materials.

Acknowledgment. The authors thank A. V. Neimark and P. I. Ravikovitch (TRI, Princeton, NJ) for providing the NDFT data. P.K. acknowledges J. Miyamoto (Chiba University, Japan) for the fruitful discussion.

LA0513609